Electron shuttles enhance phenanthrene removal in constructed wetlands filled with manganese oxides-coated sands

Xiaotong Shen [a], Jian Zhang [a,*], Huijun Xie [b], Bo Sun [a], Shuang Liang [a], Haiming Wu [a], Zhen Hu [a], Huu Hao Ngo [c], Wenshan Guo [c], Jiaxing Lu [a]

[a] Shandong Key Laboratory of Water Pollution Control and Resource Reuse, School of Environmental Science & Engineering, Shandong University, Jinan 250100, China
[b] Environment Research Institute, Shandong University, Jinan 250100, China
[c] School of Civil and Environmental Engineering, University of Technology Sydney, Broadway, NSW 2007, Australia

* Corresponding author.
E-mail address: zhangjian00@sdu.edu.cn (J. Zhang).

Keywords:
Constructed wetlands
Manganese oxides
Phenanthrene
Biochar catalyst

A B S T R A C T

Mn oxides could realize persistent organic pollutants (POPs) removal through the cycle of Mn between Mn(II) and biogenic Mn oxides in constructed wetlands (CWs) filled with Mn oxides. However, the inefficient cycle of Mn caused by the limited oxidation ability of Mn oxides inhibited its effective degradation of POPs. Ruthenium (Ru) and 2,2′-azino-bis(3-ethylbenzothiazoline)-6-sulfonate (ABTS) could act as electron shuttles in catalytic Mn oxides oxidation process. In this study, phenanthrene (PHE) was selected as a typical POP and biochar (BC) supported Ru (Ru/BC) and ABTS (ABTS/BC) were induced in CWs with Mn oxides (birnessite). The removal efficiencies of PHE in CWs with Ru/BC and ABTS/BC reached 94.61% and 95.51%, higher than the control (79.91%). ABTS performed best for enhancing Mn cycle based on the results of highest oxidation removal ca-pacity and relative abundance of Mn-oxidizing bacteria. What's more, the addition of Ru/BC contributed to the best adsorption ability and highest relative abundance of PHE degrading bacteria.

1. Introduction

With the increasing anthropogenic inputs of pollutants, such as vehicle exhausts and coal combustion, some organic pollutants were introduced in aquatic environments coming from atmospheric deposition, industrial discharge and urban runoff [1]. Constructed wetlands (CWs) as a sustainable eco-treatment system have been widely used for wastewater treatment worldwide due to its easy operation and maintenance, low operating costs, and good purification capacity [2]. These organic pollutants such as polycyclic aromatic hydrocarbons (PAHs) in aquatic environments have caused serious environmental issue due to the hyper toxicity and carcinogenic properties, which posing a serious threat to the surrounding ecological environment and human health [2]. PAHs in water tend to be set by wetland substrates due to high hydrophobicity [3]. However, most reported research only focused on adsorption and immobilization, ignoring the following degradation and removing ability of pollutants on substrates [4]. Thus, there is an urgent need for enhancing the adsorption capacity and especially the oxidation removal ability of wetland substrates as well as the synergistic effects between the chemical, physical, and biological processes, which would be extremely important for the sustainable application of CW [4].

Manganese (Mn) oxides, as a kind of common oxidants with adsorptive capability in nature, has been reported to removal clarithromycin, chlorophene, diclofenac, and triclosan in membrane bioreactors and column reactors at the lab scale water treatment processes [5]. Application of Mn oxides as a type of wetland substrate could enhance the performance of triclosan removal [6]. Accompanied with the oxidation of pollutants, Mn oxides (mostly MnO_2) were reduced to Mn(II) with or without microbial reactions [7]. Mn(II) can be further oxidized to biogenic Mn oxides by many kinds of microbes under oxygen rich conditions. This cycle of Mn between Mn (II) and biogenic Mn oxides was the crucial process for pollutants removal [8]. In addition, there are limiting factors in the process of removing organic matters from CWs with Mn oxides: (1) the weak adsorption capacity of the substrate cannot provide sufficient support for microbial degradation and oxidation of Mn oxides [9]; (2) inefficient cycle of Mn as well as the weak oxidation ability of Mn oxides for POPs which depend greatly on the surrounding conditions impedes the effective degradation of PAHs by oxidized constructed wetlands [10].

Catalyzing process of oxidation is a common method for achieving

high removal of organic matters with weak oxidation ability of oxidants. Heterogeneous catalysts could be synthesized by supporting materials and catalysts [11]. Biochar (BC) was picked as catalysts supports due to the high surface areas and large amounts of pore structures as well as the widely application for pollutants removal in CWs [12]. Among the catalysts which have potential for use in selective oxidations, ruthenium (Ru) takes a special position owing to its versatility. Ru can catalyze the oxidation of alkanes, alkenes, alcohols amines and phenols [10]. What's more, Ru could act as electron shuttle in catalytic permanganate oxidation process by the mutual transformation between high and low valences of Ru [11]. Similarly, as a simple synthetic electron shuttle, ABTS has also been widely used. For instance, several groups reported that ABTS could serve as an electron shuttle to enhance the oxidation of substituted phenols by aqueous permanganate [13]. Hence, it seems likely that Ru and ABTS can also serve as electron shuttles in the catalytic Mn oxides oxidation of POPs through the transformation of electron pairs. Electron shuttles supported on BC are expected to realized effective fixed adsorption and catalytic oxidation by solving the stability problems [14]. What's more, the synergistic effects between the chemical, physical, and biological processes are meaningful to be explored for the guidance of overall promotion of oxidized constructed wetlands [15].

In this study, an innovative method modified with Ru and ABTS embedded carbon (Ru/BC and ABTS/BC) is proposed to explore the removal and degradation pathways of phenanthrene (PHE) as the typical PAH. The objectives of this work were to: (1) elucidate whether catalysts embedded carbon, by incorporation of Ru and ABTS into biochar, could enhance the PHE removal in CWs with Mn oxides; (2) examine the performance of Ru/BC and ABTS/BC for catalyzing of birnessite oxidation and accelerating of the Mn cycle in CWs; (3) reveal the role of Ru/BC and ABTS/BC as substrate and the synergistic effects with plants and microbes in CWs.

2. Materials and methods

2.1. Chemicals and reagents

The phenanthrene and phenanthrene-d10 (>99.5% purity) used in this experiment were purchased from Aladdin Reagent (Shanghai, China). The standard substitute (p-Terphenyl-d14 and 2-fluorobiphenyl) and other chemicals of analytical grade or higher was obtained from ANPEL Laboratory Technologies (Shanghai) Inc.

Birnessite-coated sand was synthesized in batch by adding 300 g acid washed sand in 2.5 L boiling solution of 1 mol potassium permanganate. Then, 2 mol of concentrated hydrochloric acid was dropped onto the solution with vigorously stirred. After boiling for a further 10 min, the precipitate was filtered and washed with Milli-Q water. Then, 6 L birnessite-coated sand was prepared according to the above method and collected by centrifugation and dried by freeze-drying for later use [16].

2.2. Preparation and characterization of modified carbon materials

Biochar was prepared according to the previous study [17]. Afterwards, catalyst synthesis was carried out following the impregnation method reported in previous literatures [16]. For Ru/BC, a fix amount of BC was fully soaked in a saturated ruthenium chloride at a given ratio (g $RuCl_3$/g carbon; 0.05) and then dried at 105 °C for 10 h. The mixed samples were heated to 400 °C and maintained for 3 h in a muffle furnace under pure N_2 conditions. For ABTS/BC, the same impregnation ratio was implemented and the post treatment process was operated based on the method of *Katarzyna Karnicka* et al [18].

X-ray photoelectron spectrometer (XPS) measured by Thermo ESCALAB 250XI served to analyze elemental speciation of the biochar. All data were calibrated to the C1s peak of 283.9 eV [19]. X-ray diffraction (XRD) was carried out by Bruker D8 Advance to identify the structural features and the mineralogy of the catalysts. XRD data were recorded at ambient temperature on a Bruker D8 Advance powder diffractometer, in the angular range 5–70° (2θ), collected with a step of 0.02° and a step time of 8 s [5].

To validate the presence and role of catalysts served as electrons mediators, electrochemical measurements were carried out with a CS310H electrochemical workstation. A standard three-electrode cell was used. The working electrode was a glassy carbon electrode (3-mm diameter) modified with ABTS/BC. The counter electrode was made from Pt wire, and all potentials were expressed versus the Ag/AgCl (3MKCl) reference electrode (Mineral). The electrolyte solution used for these experiments was McIlvain buffer at a pH of 5.2. Prior to modification, the working electrode was polished (on a cloth) with aqueous alumina slurries (grain size, 0.5 mm) [20].

2.3. Lab-scale constructed wetland setup and operation

Eight vertical flow constructed wetlands (VFCWs) divided into two parallel groups with different application of substrates were located at Shandong University in Jinan, China (116.1°E, 36.5°N). The VFCWs reactors consisted of organic glass (60 cm in height, 20 cm in diameter). Profile and photo of experimental microcosms were shown in Fig. S1. Gravel layer (1–3 cm in diameter) was placed in the bottom layer to a height of 10 cm. The main substrate consisted of washed quartz grains (3–5 mm) to a height of 50 cm, which varied for different CW systems. Different modified biochar combined with or without birnessite-coated sand were mixed in the modified layer at the height of 20–40 cm from the bottom. The adding capacities of biochar and birnessite-coated sand were both 3 L. The 8 CW units were divided into 4 groups consisting of two pairs; units were named as follows: (1) C-CW (filled only with quartz); (2) BC-B-CW (filled with birnessite and biochar); (3) Ru/BC-B-CW (filled with birnessite and Ru-modified biochar); (4) ABTS/BC-B-CW (filled with birnessite and ABTS-modified biochar). *Iris pseudacorus* was planted with an initial density of 6 plants/unit.

VFCWs units were seeded with activated sludge collected from Everbright Water Wastewater Treatment Plant (located in Jinan, Shandong 117.0°E, 36.7°N, China) for one month before it was formally operated. After that, synthetic wastewater diluted with tap water was added to the top of the microcosm. The wastewater contained glucose, $(NH_4)_2SO_4$, KNO_3, KH_2PO_4, $MgSO_4$, $CaCl_2$, and $FeSO_4{\blacksquare}7H_2O$. A solution of PHE (1 g) dissolved in dichloromethane (1000 mL) was prepared. During the operational period certain amounts of these stock solution was added and the final concentration of PHE in the wastewater was around 0.73 μg/mL. The hydraulic retention time (HRT) lasted 3 days during the experiment period.

2.4. Sampling and analysis

Influent and effluent wastewater was collected before and after each cycle. The Chemical oxygen demand (COD), ammonia nitrogen (NH_4^+-N), nitrate nitrogen (NO_3^--N), and the Total phosphorus (TP) of the effluents were measured by standard methods [21]. The concentration of PHE was measured by Gas chromatography/mass spectrometry (GC/MS) using the internal standard method. The pretreatment and measuring methods are described in detail in our previous research [17].

In each CW unit, substrate samples of different depths (0–10 cm, 10–20 cm, 20–30 cm, 30–40 cm and 40–50 cm depth) were collected at the end of experiment for three months. Five-point sampling method was used to obtain the substrate in each depth. The plant residues were removed by sieving and the substrate samples were freeze dried for 72 h. PHE in substrate was extracted by accelerated solvent extraction with dichloromethane-methanol mixture (1:1) according to a standard method (HJ 783–2016). The plants were harvested at the end of the experimental and were separated to leaves, stems and roots. These plant samples were cut into pieces and freeze dried at − 60 °C for 72 h, after which the PHE in 10 g plant samples was extracted into 20 mL of dichloromethane and methanol at a volume ratio of 1:1 using an

accelerated solvent extraction. The extraction methods were based on the literature and standard methods [15]. Silica gel columns containing of neutral chlorine dioxide, silica gel, and Na_2SO_4 were used to purify the solution before detecting. Then the residue was reduced to the final volume of 1 mL using the vacuum concentrator (Vortex 600). GC/MS was used for the detecting of the final volume.

The microbes around the control layer and modified layer were further analyzed. Community DNA was extracted using MOBIO PowerSand™ DNA Isolation Kit (MoBio Laboratories, Inc., Carlsbad, CA, USA). DNA purity was measured using a Nanodrop ND-1000 UV–vis spectrophotometer (Nano-DropTechnologies, Wilmington, DE, USA). To obtain the desired microbial community for each substrate, Illumina high-throughput sequencing was done.

3. Results and discussion

3.1. PHE removal performance of different CWs

The concentrations of the main pollutants in the effluent reached a steady state after stabilization (Fig. 1 and S2). Throughout the experimental stage, the influent COD, NH_4^+-N, NO_3^--N, TP and PHE were approximately 69.08 mg/L, 8.23 mg/L, 12.91 mg/L, 1.55 mg/L and 0.73 mg/L, respectively. The removal rate of the NO_3^--N (96.59%) in BC-B-CW was significantly higher than that (79.41%) in C-CW. It has been demonstrated that the process of anaerobic Mn(II) oxidation coupled to nitrate reduction could enhance the denitrification [22]. The removal rates of the COD, NH_4^+-N and TP in BC-B-CW were approximately 82.99%, 83.75% and 75.34%, respectively, and in the C-CW were approximately 54.78%, 55.16%, and 14.84%, respectively. The adding of Mn oxides remarkably facilitated the pollutant removal performance of wetland microcosms. It was easy to understand that Mn oxides in a substrate could improve nitrification processes and organic carbon transformation due to their strong oxidizing properties [23]. Meanwhile, the wonderful fixation and positive effects of biochar and birnessite on plants growth and microbial compositions could also facilitate the performance of BC-B-CW [24].

Electron shuttles realized better removal performance of not only PAH but also normal pollutants. The removal of PHE in Ru/BC-B-CW and ABTS/BC-B-CW reached 94.61% and 95.51%, higher than the control (79.91%), which may be attributed to enhanced oxidizing properties of Mn oxides. Dramatically promotion of TP removal was also observed (Fig. S2d). The removal rates of TP in Ru/BC-B-CW (92.90%) and ABTS/BC-B-CW (94.45%) was significantly higher than that (75.48%) in BC-B-CW system. The predominant form of P in wastewater effluent is anionic [25]. Immobilized particles of a metal cation in substrates typically form the polymer exchange base, termed a polymeric ligand exchanger, by which P anions in wastewater could be easier selected than other "competing" ions, such as sulfates or chlorides [26]. Interestingly, the introduction of electrons mediators facilitated the biological P removal according to the results of high-throughput sequencing: the relative abundances of *Candidatus Accumulibacter phosphatis* (Accumulibacter), the most widely studied phosphorus-accumulating organisms (PAO) [25], in Ru/BC-B-CW and ABTS/BC-B-CW were 2.52 times and 3 times respectively more than that of BC-B-CW. More available electron acceptors of modified biochar are considered key contributors due to the enhanced metabolic pathways of PAO in the aerobic phase. They could oxidize carbon source and the subsequent energy release is used for the uptake of P (with stabilizing cations) [27].

3.2. The role of substrate for PHE removal

Based on the settling characteristics of PAHs, the concentrations of PHE at different depths of the substrate (0–10 cm, 10–20 cm, 20–30 cm, 30–40 cm and 40–50 cm depth) were studied at the end of the experiment (Fig. 1b). The PHE accumulated in the substrate in the CWs in the following order: C-CW (2.84 ± 0.14 μg/g) > BC-B-CW (2.19 ± 0.08 μg/g) > Ru/BC-B-CW (0.79 ± 0.05 μg/g) > ABTS/BC-B-CW (0.70 ± 0.05 μg/g). Different matrix compositions caused variation of pollutant distribution. Among the different substrate depths, C-CW performed the highest PHE contents at 0–10 cm depth, i.e., 0.82 ± 0.03 μg/g, indicating that the PHE in CWs could remain in the superficial substrate instead of undergoing precipitation in the deep layer. By contrast, it indicated that birnessite could contribute to the migration of PHE to the deep substrate, especially the modified layer, and promote the integral pollutants removal efficiency of vertical flow constructed wetlands. It could be found that birnessite also contributed to the remove of PHE. C-CW has the highest PHE contents in each depth of substrate layer. The amounts of PHE in 0–10 cm depth of BC-B-CW, Ru/BC-B-CW and ABTS/BC-B-CW were 75.74%, 85.78% and 89.34% respectively lower than that of C-CW. This significant decrease can be related to the birnessite, which can enhance pollutant accumulation in plants and thus decrease the PHE contents in the rhizosphere substrate. Similarly, in deeper depth, BC-B-CW, Ru/BC-B-CW and ABTS/BC-B-CW performed obviously lower accumulation of PHE due to the oxidation of Mn oxides.

Mn oxides have oxidation ability and adsorptive capability as well as biochar primarily due to their large specific surface areas and small particle sizes [23]. To reveal the mechanism of enhanced pollutants removal with birnessite catalyzed by redox mediators embedded carbon, decay of PHE (5 μM) by matrix with different compositions were performed in well-closed, light-resistant reaction systems with microbial inactivation to avoid the effects of photolyzes, volatilization and

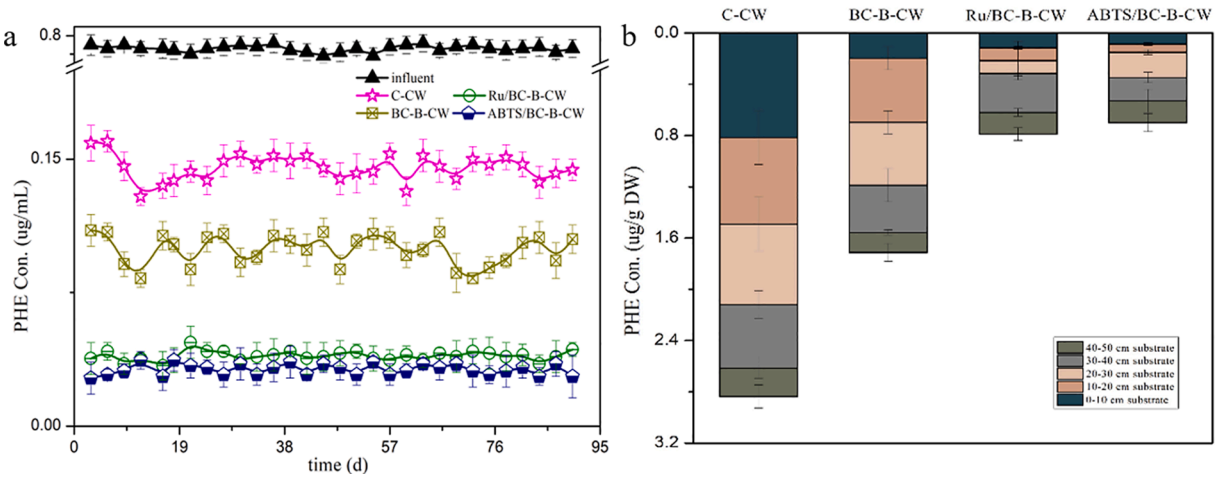

Fig. 1. Concentrations of PHE in each microcosm (a) and contents of PHE of substrates in different depths of CWs.

microorganisms. As shown in Fig. 2, the removal of PHE by matrix consisted of oxidation–reduction and physical absorption. At the initial stage, the contents of PHE fixation on matrix dramatically increased. The substrates of Ru/BC-B performed highest fixed capacity of 9.92 μg/g, which was 2.86 times and 2.95 times respectively more than that of BC-B and ABTS/BC-B. The loading of metal ions on the surface of the biochar could maximize the PAH adsorption ability by complexation complex absorption, hydrophobic adsorption, and electrostatic attraction [28]. The fixing contents of PHE on substrates reduced as the reaction progress, which was attributed to the chemical degradation by Mn oxides. What's more, it could be concluded that the pollutants removal by substrates with Mn oxides was mainly dependent on oxidation–reduction. Both redox mediators realized chemical catalytic action for Mn oxidation. Among these three different substrates compositions, ABTS/BC-B performed the best oxidation–reduction ability with oxidation removal capacity of 5.47 mg, 29.31% and 17.38% higher than that of BC-B and Ru/BC-B.

3.3. Electrons transformation on biochar settled with electrons shuttles

To explore the catalytic process of Ru/BC catalyst systems, chemical state information was obtained by XPS analysis of both the Ru(3d) and the lesser-studied Ru(3p) core levels because of the overlap of the C(1s) and Ru(3d) core levels [29]. For the used catalysts, there is a clear shift in the binding energies toward lower energy which may be caused by an increase in the mean particle size. The final Ru(3p) energy of 464.9 eV revealed the formation of metallic ruthenium or RuOx/Ru and further supported by the Ru(3d) value of 282 eV (Fig. 3a and b) [30]. The multivalent Ru species (Ru and RuO_2) on used BC confirmed the excellent reversible redox transition performance based on the fast transformation of Ru and promote redox reactions of Ru (Ru-RuO_2) with Mn oxides. As shown in Fig. 3c, the Ru^{4+}/Ru^0 atomic ratios have an obvious reduction after the test, indicating that the amount of oxygen vacancies decreases.

For ABTS/BC catalyst systems, the cyclic voltametric response was used to demonstrate the performance of catalyst. For comparison, cyclic voltammograms of ABTS adsorbate on bare glassy carbon and ABTS dissolved in solution (Fig. 3d) are provided. A pair of highly reversible redox peaks of ABTS centering at 0.443 V was observed at the bare GC electrode, which should be correlated with the reversible redox between $ABTS^{2-}$ and $ABTS^{\cdot-}$ [20]. The presence of adsorbed ABTS on BC is evident from cyclic voltametric responses of ABTS-modified BC deposited on glassy carbon (Fig. 3e). A pair of well-defined redox peaks for ABTS attached to BC was also observed at 0.462 V. A slightly negative potential shift (~19 mV) has been observed for ABTS adsorbed on BC and dissolved in solution due to some specific (oxidative) interactions of ABTS with BC surfaces.

The peak currents were proportional to scan rate (n) up to 400 mV/s (Fig. 3f), consistent with the surface-type behavior of the system, which also indicates that the electron transfer here is fast. The immobilized ABTS can be quantified from the slope of the curve. The interfacial population of ABTS in the case of ABTS/BC modified GC electrode the interfacial population of ABTS is 2.89×10^{-8} mol/cm^2. We have also checked the stability of the film of ABTS/BC modified GC electrode. As shown in Fig. 4b, the long-term potential cycling at 50 mV/s for 500 cycles barely resulted in any changes in the voltametric characteristics of the system. Based on the above findings, superior PHE removal performance of stable mediating system with ABTS/BC was contributed to charge propagation capabilities of ABTS/BC.

3.4. Enhanced Mn cycle

To reveal the positive role and catalytic process of electron shuttles for PHE removal, the proposed catalytic process of Mn cycle was illustrated as the conceptual model in Fig. S3. The enhanced reversible electron transformation process of electron shuttles has been confirmed above, providing better reaction condition for the Mn oxidation. XRD and XPS analyses were used to demonstrate the process of Mn cycle. Compared with substrate before experiment, peaks of XRD pattern were appeared differently at substrate modified layer in CWs, which were related to changed composition of manganese compounds (Fig. S4). In order to illuminate Mn redox cycles in different CW units, comparison of contents of various Mn species, average Mn oxidation states and the binding energy of electron energy levels (i.e., Mn2p and Mn3s) were tease out in Fig. 4 based on XPS analyses (Fig. 4a–d). According to the comparison with literature data, Mn oxides has been synthesized in three different main oxidation states, as MnO (MnII), Mn_2O_3 (MnIII), and MnO_2 (MnIV) [31]. The variations of Mn(II), Mn(III), and Mn(IV) relative amounts were detected and a common approach was used to determine the average oxidation state of Mn oxides by evaluating the peak binding energy distance in the multiplet split Mn 3 s region (Fig. S5 and Table S2). It could be found that composition ratio of highly-charged components Mn(IV) and Mn(III) intermediates increased in all CW units after experiment. Highly-charged components increased most in CWs with electron shuttles. The induce of electrons shuttles enhanced the average Mn oxidation state, which was positively correlated with the rate of chemical reaction. Compared with oxidation of organic pollutants, the oxidation of electron shuttles was much easier, decreasing the consumption of highly-charged Mn components. Meanwhile, removing of pollutants was enhanced by electron shuttles with higher reactivity [32]. What's more, as a kind of controlling specifications of water

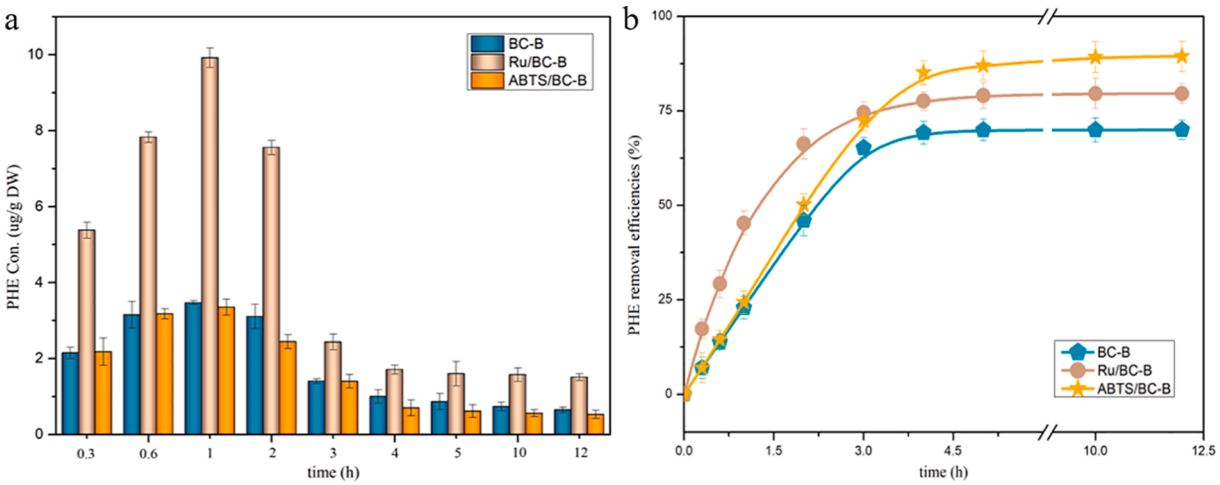

Fig. 2. Contents of fixed PHE (a) and removal efficiencies (b) of PHE (5 μM) with different substrates.

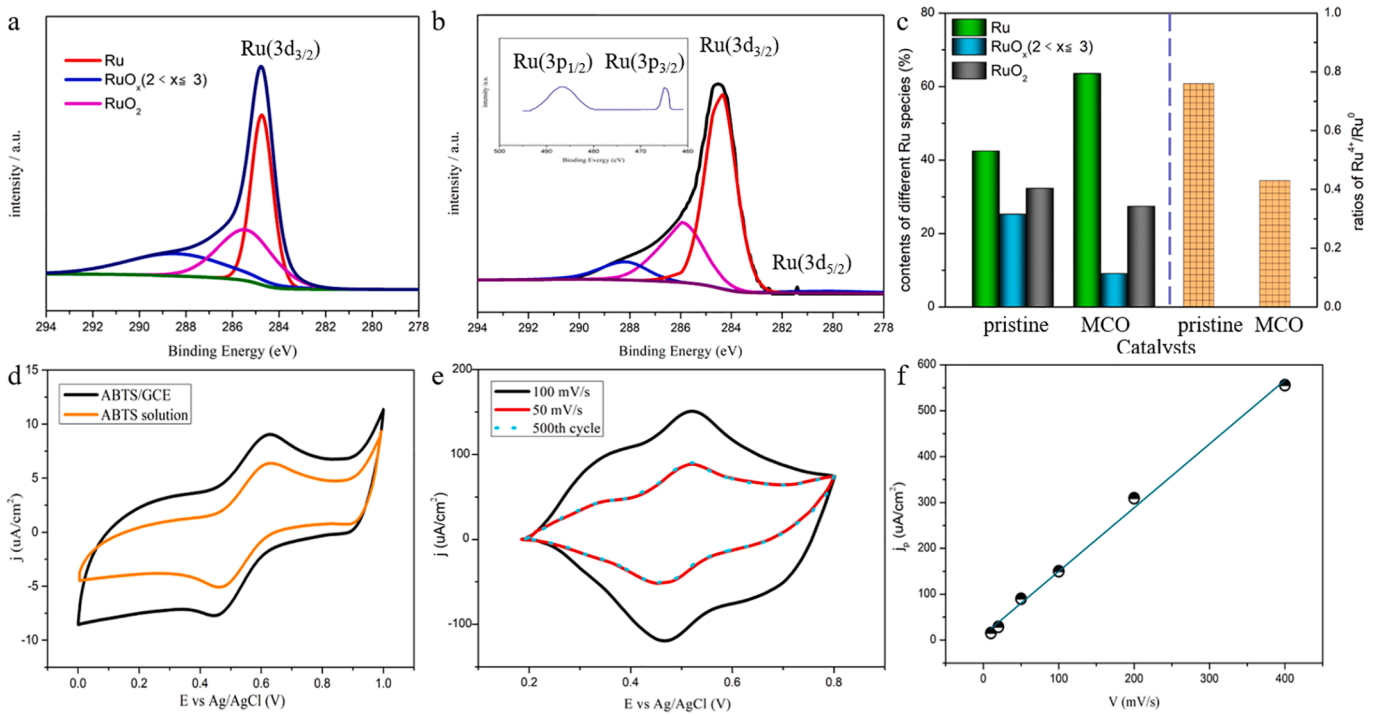

Fig. 3. Ru core-level spectra for the Ru/BC (a) before the experiment; (b) at modified layer of post-experiment; (c) comparison of contents of various Ru species and Ru^{4+}/Ru^{0} for pristine and biochar after Mn catalytic oxidation; (d) cyclic voltametric (CV) responses of 0.2 mM ABTS solution and ABTS modified glassy carbon electrode (GCE); (e) ABTS modified BC deposited on glassy carbon at 100 mV/s and 50 mV/s with recorded following long-term (500 cycles) voltametric potential cycling; (f) illustrates the dependence of the reduction peak current on scan rate.

quality, Mn^{2+} concentrations in finally effluents were also measured. All of the Mn^{2+}(aq) concentrations below 0.05 mg/L, bellowing the US EPA water quality criteria (0.05 mg/L) [33].

Mn-oxidizing bacteria play an important role in the process of Mn cycle (the electron transfer process e in Fig. S3). Besides, the synergistic effects between substrates of different components and wetland microorganisms were also essential for the performance of wetland. The Illumina high-throughput results for 16S rRNA gene sequencing data were used to evaluate the microbial community in control layer and modified layer. There was little difference on microbial species richness between modified layers of different CW units as well as the control layer in the same unit (Table S3). However, it could be found that the main metabolic process and function of microbe in different CW units were very different. Tax4Fun was used to predict the functional content of microorganism and the heatmap of metabolic functional diversity was given in Fig. 4e. The metabolic function of wetland substrate bacteria was mainly clustered to the chemoheterotrophy, nitrate reduction, nitrate respiration, nitrogen respiration, nitrite respiration and aromatic hydrocarbon degradation, indicating to chemoheterotrophy process and the removal of NO_3^--N and PHE. What's more, iron respiration was also found in CWs with electron shuttles, which indicated the formation of Fe cycle with the iron ions in synthetic wastewater. This result explained the phenomenon of additional Fe on the surface of birnessite after the experiment (Table S1). Fe cycle is also an important element cycle process in nature, and it could also realize pollutants removal just like Mn cycle.

The relative abundance of Mn-oxidizing bacteria, Fe-oxidizing bacteria and PAH degradation genera were shown in Fig. 4f-h. There was a considerable difference of relative abundance of Mn-oxidizing microbes in modified layers in different CW units. The total relative abundance of Mn-oxidizing bacteria was highest with the CWs containing ABTS/BC-B, which was 1.72 and 3.58 times more than Ru/BC-B-CW and BC-B-CW (Fig. 4f). This result coincides with the enhanced catalytic oxidation of Mn oxides by ABTS/BC, reflecting that ABTS performed best for PHE removal by Mn cycle. As shown in Fig. 4g, units with catalysts shown relatively higher abundance of Fe-oxidizing microbes. The amount of Fe-oxidizing microbes in ABTS/BC-B-CW was 19.16% and 38.97% higher than that in Ru/BC-B-CW and BC-B-CW, coinciding with the best catalytic action of ABTS. It could be concluded that ABTS performed best for enhancing element cycle of Mn and Fe.

Researchers have reported several microorganisms with the potential to biodegrade PAH such as *Acinetobacter*, *Acidovorax*, *Nitrosomonas*, *Paenibacillus*, *Alcaligenes*, *Corynebacterium*, *Vibrio*, *Methylobacillus*, *Comamonas*, *Nocardioides*, *Chryseobacterium*, *Sphingomonas*, *Mycobacterium*, *Staphylococcus*, *Flavobacterium*, *Aeromonas*, *Streptomyces*, *Pseudoxanthomonas* and *Micrococcus* [3,34–37]. The total relative abundance of PAH degrading bacteria in Ru/BC-B-CW accounted for 5.89% of all detected microbial organisms, which was 106.67% and 180.48% higher than that of ABTS/BC-B-CW and BC-B-CW. The enhanced adsorption ability of Ru/BC-B through complex absorption, hydrophobic adsorption, and electrostatic attraction offered better reaction condition for the microbial degradation of PAH [37].

3.5. *Transformation pathways and removal mechanism of PHE in CWs*

Identification products of PHE was performed through GC-MS analysis to reveal the transformation pathways for the degradation of PHE. Proposed catabolic pathway of PHE in CW with Mn oxides catalysted by catalysts was given in Fig. 5. In these CW systems, macrophyte, microflora and substrates with Mn oxides are the characteristic feature of wetlands. The intensive biological activities in such an ecosystem lead to a high rate of autotrophic and heterotrophic processes. Mn oxides is considered as the major oxidizing species, which can preferentially attack PHE at positions 9 and 10 to yield theoretical products 9, 10-phenanthrene intermediate (product 1) [38]. Further oxidation leads to 1-hydroxy-2-naphthoic acid (product 2), which was an intermediate metabolite in PHE degradation indicating the presence of bacterial microflora. Then, these intermediates formed trans-2-

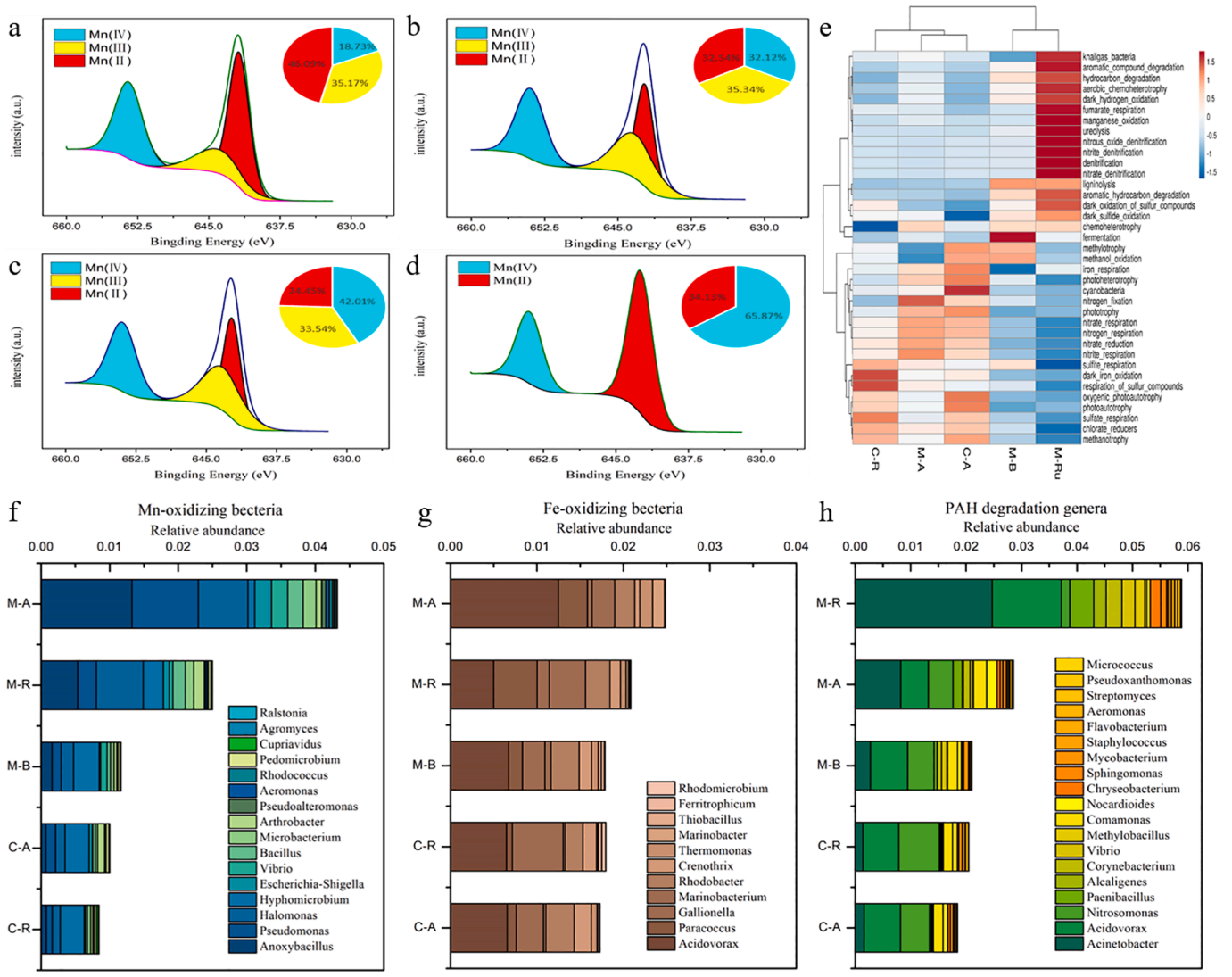

Fig. 4. The XPS spectra of Mn2p for birnessite before the experiment (a) and birnessite in different operated CW units: BC-B-CW (b), Ru/BC-B-CW (c) and ABTS/BC-B-CW (d). Metabolic functional diversity of bacterial community structure (e) and relative abundances of Mn-oxidizing bacteria, Fe-oxidizing bacteria and PAH degradation genera in the substrate. (M-B: modified layer in BC-B-CW; M-R: modified layer in Ru/BC-B-CW; M-A: modified layer in ABTS/BC-B-CW; C-R: control layer in Ru/BC-B-CW; C-A: control layer in ABTS/BC-B-CW).

carboxybenzalpyruvic acid (product 3) and were cleared by TCA cycle based on the observation of phthalic acid (product 4) [39].

The mechanism of pollutant removal in CW with birnessite catalyzed by electron shuttles on biochar was also proposed. The adding of birnessite realized effective promotion of oxidizing property and boosted the migration of PHE with high hydrophobicity [40]. In the modified layer, excellent adsorptive capability of birnessite and biochar enhanced the fixation of PHE, providing better condition for the following catalytic oxidation and microbial degradation. Mn cycle was enhanced by ABTS/BC and Ru/BC served as efficient electron shuttles with excellent proton transfer ability and superior reversible redox transition performance. PHE and some other pollutants served as electron acceptors to be degraded by chemical oxidation of Mn oxides [41]. Plant absorption and microbial degradation were improved by modified substrates based on the synergistic effects between these three main components of wetland. The pollutants uptake by plants in CW with Mn oxides was also observed by detecting the PHE contents in roots, stems and leaves of plants (Fig. S6). The total PHE accumulation in the plants of C-CW (99.6 μg) was much lower compared with the other treatments, the average value of which was 229.43 μg. What's more, the increasing adsorption ability of Ru/BC boosted PHE microbial degradation [42]. In brief, electron shuttles could boost oxidation susceptibility of CW with Mn cycle, as well as Fe cycle and enhance wetland performance based on the synergistic effects between important components of wetland.

4. Conclusions

Enhanced removal of PHE and other pollutants in CWs with Mn oxides catalyzed by electron shuttles was obtained via improved Mn cycle. Mn cycle was revealed by the results of XPS, XRD and analysis of Mn-oxidizing bacteria. Catalytic process of Ru/BC and ABTS/BC was revealed by the formation of electron pairs and excellent charge propagation capabilities which boosted the oxidation–reduction reaction between substrates with pollutants. The best oxidation removal capacity of PHE and highest total relative abundance of Mn-oxidizing bacteria demonstrated that ABTS/BC performed best for enhancing Mn cycle. However, the addition of Ru/BC contributed to the best adsorption ability and highest relative abundance of PHE degrading bacteria. What's more, the induced electron shuttles combined with iron ions formed Fe cycle based on the results of metabolic functional diversity of bacterial community structure and the higher abundance of Fe-oxidizing microbes. In conclusion, electron shuttles could boost oxidation

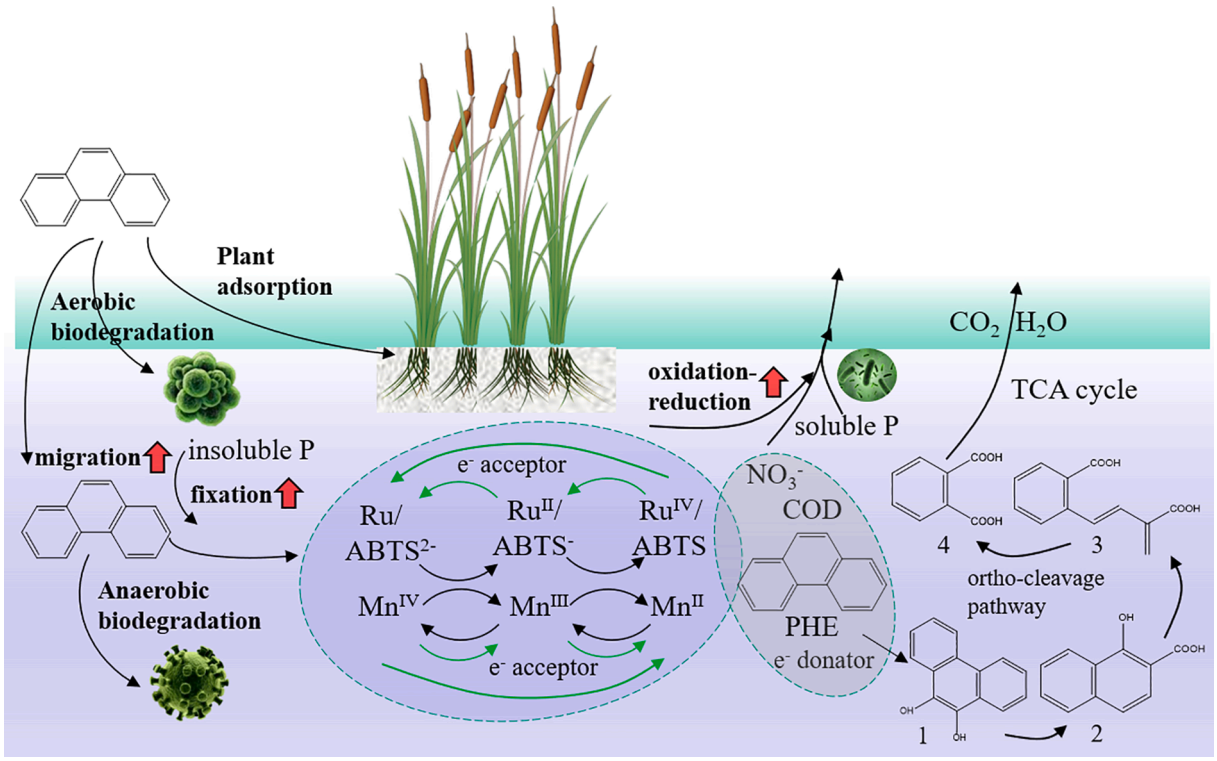

Fig. 5. Transformation pathway and removal mechanism for the degradation of PHE in CW.

susceptibility of CW with Mn cycle, as well as the adsorptive capacities and microbial degradation.

Declaration of Competing Interest

The authors declare that they have no known competing financial interests or personal relationships that could have appeared to influence the work reported in this paper.

Acknowledgements

This work received supports from National Science Foundation for Distinguished Young Scholar of China (No. 51925803), National Natural Science Foundation of China (No. 51720105013, 51978385), Shandong Provincial Key Research and Development Program (Major Scientific and Technological Innovation Project) (No. 2019JZZY010411, 2020CXGC011406).

Appendix A. Supplementary data

Supplementary data to this article can be found online at https://doi. org/10.1016/j.cej.2021.131755.

References

[1] C. Avila, J.M. Bayona, I. Martin, J. Jose Salas, J. Garcia, Emerging organic contaminant removal in a full-scale hybrid constructed wetland system for wastewater treatment and reuse, Ecol. Eng. 80 (2015) 108–116. https://doi.org/10.1016/j.ecoleng.2014.07.056.

[2] H.I. Abdel-Shafy, M.S.M. Mansour, A review on polycyclic aromatic hydrocarbons: Source, environmental impact, effect on human health and remediation, Egypt. J. Pet. 25 (1) (2016) 107–123, https://doi.org/10.1016/j.ejpe.2015.03.011.

[3] M. Ahmad, Q. Yang, Y. Zhang, J. Ling, W. Sajjad, S. Qi, W. Zhou, Y. Zhang, X. Lin, Y. Zhang, J. Dong, The distinct response of phenanthrene enriched bacterial consortia to different PAHs and their degradation potential: a mangrove sediment microcosm study, J. Hazard. Mater. 380 (2019) 120863, https://doi.org/10.1016/j.jhazmat.2019.120863.

[4] K. Bao, C. Zaccone, Y. Tao, J. Wang, J.i. Shen, Y. Zhang, Source apportionment of priority PAHs in 11 lake sediment cores from Songnen Plain, Northeast China, Water Res. 168 (2020) 115158, https://doi.org/10.1016/j.watres.2019.115158.

[5] A.A. Akinpelu, M.E. Ali, M.R. Johan, R. Saidur, M.A. Qurban, T.A. Saleh, Polycyclic aromatic hydrocarbons extraction and removal from wastewater by carbon nanotubes: A review of the current technologies, challenges and prospects, Process Saf. Environ. Prot. 122 (2019) 68–82, https://doi.org/10.1016/j.psep.2018.11.006.

[6] J. Jiang, Z. Wang, Y. Chen, A. He, J. Li, G.D. Sheng, Metal inhibition on the reactivity of manganese dioxide toward organic contaminant oxidation in relation to metal adsorption and ionic potential, Chemosphere 170 (2017) 95–103, https://doi.org/10.1016/j.chemosphere.2016.12.015.

[7] H. Xie, Y. Yang, J. Liu, Y. Kang, J. Zhang, Z. Hu, S. Liang, Enhanced triclosan and nutrient removal performance in vertical up-flow constructed wetlands with manganese oxides, Water Res. 143 (2018) 457–466, https://doi.org/10.1016/j.watres.2018.05.061.

[8] S. Balgooyen, P.J. Alaimo, C.K. Remucal, M. Ginder-Vogel, Structural transformation of MnO2 during the oxidation of bisphenol A, Environ. Sci. Technol. 51 (11) (2017) 6053–6062, https://doi.org/10.1021/acs.est.6b0590410.1021/acs.est.6b05904.s001.

[9] I. Forrez, M. Carballa, K. Verbeken, L. Vanhaecke, M. Schluesener, T. Ternes, N. Boon, W. Verstraete, Diclofenac oxidation by biogenic manganese oxides, Environ. Sci. Technol. 44 (9) (2010) 3449–3454, https://doi.org/10.1021/es9027327.

[10] C.-D. Dong, C.-W. Chen, C.-M. Hung, Synthesis of magnetic biochar from bamboo biomass to activate persulfate for the removal of polycyclic aromatic hydrocarbons in marine sediments, Bioresour. Technol. 245 (2017) 188–195, https://doi.org/10.1016/j.biortech.2017.08.204.

[11] X. Zhang, T. Yu, X. Li, J. Yao, W. Liu, S. Chang, Y. Chen, The fate and enhanced removal of polycyclic aromatic hydrocarbons in wastewater and sludge treatment system: A review, Crit. Rev. Environ. Sci. Technol. 49 (16) (2019) 1425–1475, https://doi.org/10.1080/10643389.2019.1579619.

[12] P. Azadi, R. Farnood, Review of heterogeneous catalysts for sub- and supercritical water gasification of biomass and wastes, Int. J. Hydrogen Energy 36 (16) (2011) 9529–9541, https://doi.org/10.1016/j.ijhydene.2011.05.081.

[13] J. Zhang, B. Sun, X. Guan, H. Wang, H. Bao, Y. Huang, J. Qiao, G. Zhou, Ruthenium nanoparticles supported on CeO2 for catalytic permanganate oxidation of butylparaben, Environ. Sci. Technol. 47 (22) (2013) 13011–13019, https://doi.org/10.1021/es402118v.

[14] X. Yang, Q. He, F. Guo, X. Sun, J. Zhang, Y.i. Chen, Impacts of carbon-based nanomaterials on nutrient removal in constructed wetlands: Microbial community structure, enzyme activities, and metabolism process, J. Hazard. Mater. 401 (2021) 123270, https://doi.org/10.1016/j.jhazmat.2020.123270.

[15] S. Muhammad, P.R. Shukla, M.O. Tade, S. Wang, Heterogeneous activation of peroxymonosulphate by supported ruthenium catalysts for phenol degradation in water, J. Hazard. Mater. 215 (2012) 183–190, https://doi.org/10.1016/j.jhazmat.2012.02.045.

[16] Y. Kang, H. Xie, B. Li, J. Zhang, H.H. Ngo, W. Guo, Z. Gun, Q. Kong, S. Liang, J. Liu, T. Cheng, L. Zhang, Performance of constructed wetlands and associated mechanisms of PAHs removal with mussels, Chem. Eng. J. 357 (2019) 280–287, https://doi.org/10.1016/j.cej.2018.09.152.
[17] R.M. McKenzie, The surface-charge on manganese dioxides, Aust. J. Soil Res. 19 (1) (1981) 41–50, https://doi.org/10.1071/sr9810041.
[18] X. Shen, J. Zhang, H. Xie, Z. Hu, S. Liang, H.H. Ngo, W. Guo, X. Chen, J. Fan, C. Zhao, Intensive removal of PAHs in constructed wetland filled with copper biochar, Ecotoxicol. Environ. Saf. 205 (2020) 111028, https://doi.org/10.1016/j.ecoenv.2020.111028.
[19] K. Karnicka, K. Miecznikowski, B. Kowalewska, M. Skunik, M. Opallo, J. Rogalski, W. Schuhmann, P.J. Kulesza, ABTS-modified multiwalled carbon nanotubes as an effective mediating system for bioelectrocatalytic reduction of oxygen, Anal. Chem. 80 (19) (2008) 7643–7648, https://doi.org/10.1021/ac8011297.
[20] H. Radinger, P. Connor, R. Stark, W. Jaegermann, B. Kaiser, Manganese oxide as an inorganic catalyst for the oxygen evolution reaction studied by X-ray photoelectron and operando Raman spectroscopy, ChemCatChem 13 (4) (2021) 1175–1185, https://doi.org/10.1002/cctc.v13.410.1002/cctc.202001756.
[21] W. Deng, Y. Tan, Z. Fang, Q. Xie, Y. Li, X. Liang, S. Yao, ABTS-multiwalled carbon nanotubes nanocomposite/Bi film electrode for sensitive determination of Cd and Pb by differential pulse stripping voltammetry, Electroanalysis 21 (22) (2009) 2477–2485, https://doi.org/10.1002/elan.200900207.
[22] F.W. Gilcreas, Future of standard methods for examination of water and wastewater, Health Laboratory Sci. 4 (3) (1967) 137–1000.
[23] D. Swathi, P.C. Sabumon, S.M. Maliyekkal, Microbial mediated anoxic nitrification-denitrification in the presence of nanoscale oxides of manganese, Int. Biodeterior. Biodegrad. 119 (2017) 499–510, https://doi.org/10.1016/j.ibiod.2016.10.043.
[24] M. Huguet, M. Deborde, S. Papot, H. Gallard, Oxidative decarboxylation of diclofenac by manganese oxide bed filter, Water Res. 47 (14) (2013) 5400–5408, https://doi.org/10.1016/j.watres.2013.06.016.
[25] H. Schulz, G. Dunst, B. Glaser, Positive effects of composted biochar on plant growth and soil fertility, Agron. Sustainable Dev. 33 (4) (2013) 817–827, https://doi.org/10.1007/s13593-013-0150-0.
[26] J.T. Bunce, E. Ndam, I.D. Ofiteru, A. Moore, D.W. Graham, A review of phosphorus removal technologies and their applicability to small-scale domestic wastewater treatment systems, Front. Environ. Sci. 6 (2018), https://doi.org/10.3389/ fenvs.2018.00008.
[27] C.A. Arias, M. Del Bubba, H. Brix, Phosphorus removal by sands for use as media in subsurface flow constructed reed beds, Water Res. 35 (5) (2001) 1159–1168, https://doi.org/10.1016/s0043-1354(00)00368-7.
[28] B. Acevedo, A. Oehmen, G. Carvalho, A. Seco, L. Borras, R. Barat, Metabolic shift of polyphosphate-accumulating organisms with different levels of polyphosphate storage, Water Res. 46 (6) (2012) 1889–1900, https://doi.org/10.1016/j.watres.2012.01.003.
[29] M. Ahmad, A.U. Rajapaksha, J.E. Lim, M. Zhang, N. Bolan, D. Mohan, M. Vithanage, S.S. Lee, Y.S. Ok, Biochar as a sorbent for contaminant management in soil and water: A review, Chemosphere 99 (2014) 19–33, https://doi.org/10.1016/j.chemosphere.2013.10.071.
[30] S. Iqbal, S.A. Kondrat, D.R. Jones, D.C. Schoenmakers, J.K. Edwards, L. Lu, B. R. Yeo, P.P. Wells, E.K. Gibson, D.J. Morgan, C.J. Kiely, G.J. Hutchings, Ruthenium nanoparticles supported on carbon: an active catalyst for the hydrogenation of lactic acid to 1,2-propanediol, ACS Catal. 5 (9) (2015) 5047–5059, https://doi.org/10.1021/acscatal.5b00625.
[31] T. Fovanna, S. Campisi, A. Villa, A. Kambolis, G. Peng, D. Rentsch, O. Krocher, M. Nachtegaal, D. Ferri, Ruthenium on phosphorous-modified alumina as an effective and stable catalyst for catalytic transfer hydrogenation of furfural, RSC Adv. 10 (19) (2020) 11507–11516, https://doi.org/10.1039/d0ra00415d.
[32] E.S. Ilton, J.E. Post, P.J. Heaney, F.T. Ling, S.N. Kerisit, XPS determination of Mn oxidation states in Mn (hydr)oxides, Appl. Surf. Sci. 366 (2016) 475–485, https://doi.org/10.1016/j.apsusc.2015.12.159.
[33] Y. Song, J. Jiang, J. Ma, S.-Y. Pang, Y.-Z. Liu, Y. Yang, C.-W. Luo, J.-Q. Zhang, J. Gu, W. Qin, ABTS as an electron shuttle to enhance the oxidation kinetics of substituted phenols by aqueous permanganate, Environ. Sci. Technol. 49 (19) (2015) 11764–11771, https://doi.org/10.1021/acs.est.5b03358.
[34] K. Yuan, B. Chen, Q. Qing, S. Zou, X. Wang, T. Luan, Polycyclic aromatic hydrocarbons (PAHs) enrich their degrading genera and genes in human-impacted aquatic environments, Environ. Pollut. 230 (2017) 936–944, https://doi.org/10.1016/j.envpol.2017.07.059.
[35] S. Sun, Y. Wang, T. Zang, J. Wei, H. Wu, C. Wei, G. Qiu, F. Li, A biosurfactant-producing Pseudomonas aeruginosa S5 isolated from coking wastewater and its application for bioremediation of polycyclic aromatic hydrocarbons, Bioresource Technology 281 281 (2019) 421–428, https://doi.org/10.1016/j.biortech.2019.02.087.
[36] J. Li, C. Luo, G. Zhang, D. Zhang, Coupling magnetic-nanoparticle mediated isolation (MMI) and stable isotope probing (SIP) for identifying and isolating the active microbes involved in phenanthrene degradation in wastewater with higher resolution and accuracy, Water Res. 144 (2018) 226–234, https://doi.org/10.1016/j.watres.2018.07.036.
[37] S. Llado, S. Covino, A.M. Solanas, M. Petruccioli, A. D'Annibale, M. Vinas, Pyrosequencing reveals the effect of mobilizing agents and lignocellulosic substrate amendment on microbial community composition in a real industrial PAH-polluted soil, J. Hazard. Mater. 283 (2015) 35–43, https://doi.org/10.1016/j.jhazmat.2014.08.065.
[38] J. Carlos Moreno-Pirajan, J. Tirano, B. Salamanca, L. Giraldo, Activated carbon modified with copper for adsorption of propanethiol, Int. J. Mol. Sci. 11(3) (2010)
927-942. https://doi.org/10.3390/ijms11030927.
[39] J.-S. Seo, Y.-S. Keum, Q.X. Li, Mycobacterium aromativorans JS19b1(T) degrades phenanthrene through C-1,2, C-3,4 and C-9,10 dioxygenation pathways, Int. Biodeterior. Biodegrad. 70 (2012) 96–103, https://doi.org/10.1016/j.ibiod.2012.02.005.
[40] A.K. Haritash, C.P. Kaushik, Biodegradation aspects of Polycyclic Aromatic Hydrocarbons (PAHs): A review, J. Hazard. Mater. 169 (1–3) (2009) 1–15, https://doi.org/10.1016/j.jhazmat.2009.03.137.
[41] A. Dutt Tripathi, V. Paul, A. Agarwal, R. Sharma, F. Hashempour-Baltork, L. Rashidi, K. Khosravi Darani, Production of polyhydroxyalkanoates using dairy processing waste - A review, Bioresour. Technol. 326 (2021) 124735, https://doi.org/10.1016/j.biortech.2021.124735.
[42] L. Jia, H. Liu, Q. Kong, M. Li, S. Wu, H. Wu, Interactions of high-rate nitrate reduction and heavy metal mitigation in iron-carbon-based constructed wetlands for purifying contaminated groundwater, Water Res. 169 (2020) 115285, https://doi.org/10.1016/j.watres.2019.115285.